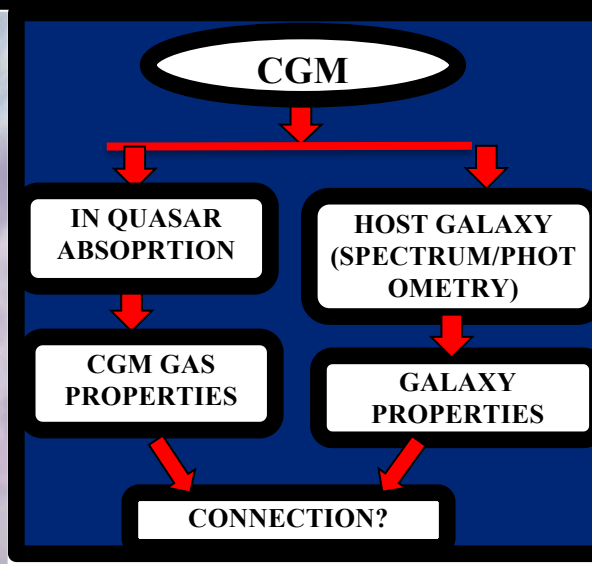
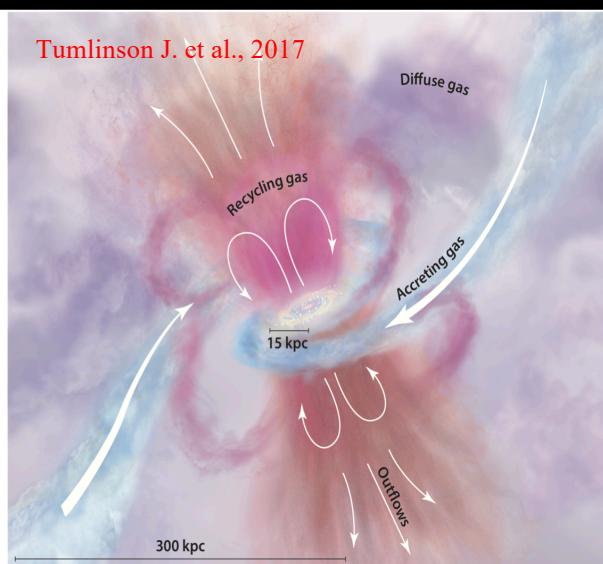


INTRODUCTION

Circumgalactic Medium (CGM):

- Diffuse Gas surrounding galaxy but outside the disk or interstellar medium and inside its virial radii.
- Observed mostly in absorptions



- Encompass most of the missing metals from the host galaxy.

DATA

- Absorbers: High-z ($2.0 \leq z \leq 3.3$): VLT/UVES and KECK/HIRES - well resolved. Low-z ($0.2 \leq z \leq 0.9$): HST/COS - unlike high-z, at low-z one will be able to map the gas and galaxy distribution as galaxy surveys will also be complete.
- Galaxies: Primarily SDSS DR16 catalog. Cross matched with other available optical/UV/IR observations.

MODELS

- We use CLOUDY (Ferland G. J., et al. 2017) for our photoionization models with the recently updated Khaire & Srianand 2019 extragalactic background as the incident radiation.

RESULTS AND DISCUSSIONS

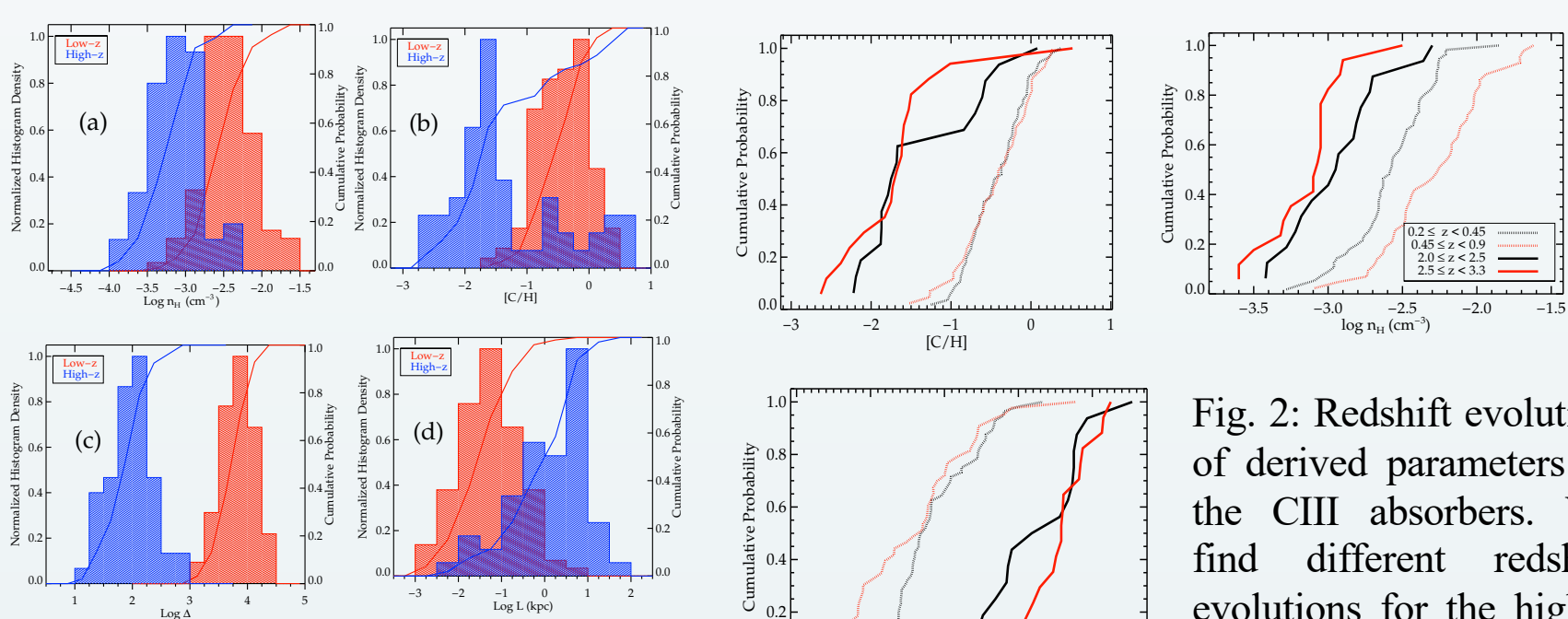


Fig. 1: Histogram of derived parameters of the C III absorbers: (a) number density (n_H), (b) carbon abundances ($[C/H]$), (c) overdensity (Δ) and (d) line of sight thickness of the absorbers (L).

Mohapatra A. et al., 2019, MNRAS, 484, 5028

Mohapatra A. et al., 2021, MNRAS, 501, 5424

➤ C III absorbers show similar properties of gas that are originating from diffuse CGM.

➤ Statistically significant redshift evolution of derived parameters between high-z and low-z

SIZE-METALLICITY RELATION

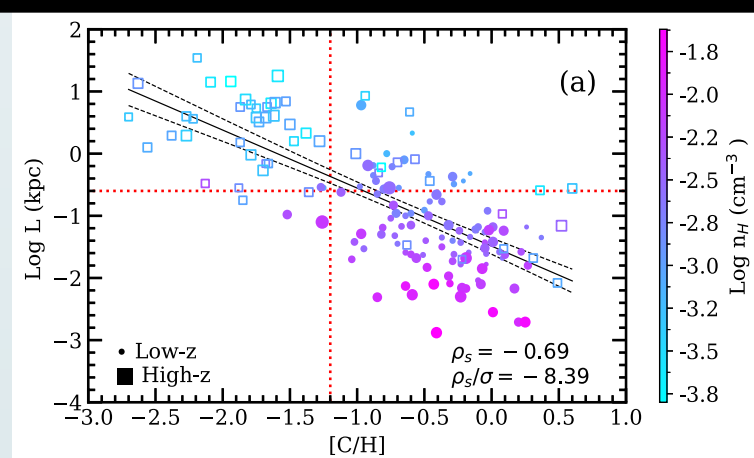
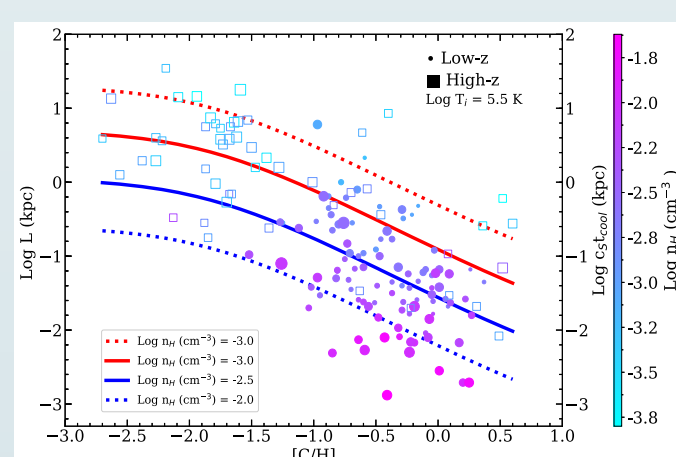


Fig. 3: Strong correlation of size and metallicity

Mohapatra A. et al. 2021, MNRAS, 501, 5424

Fig. 4: Explainable with a simple model of cooling time scale



BIOMODALITY IN C III ABSORBERS?

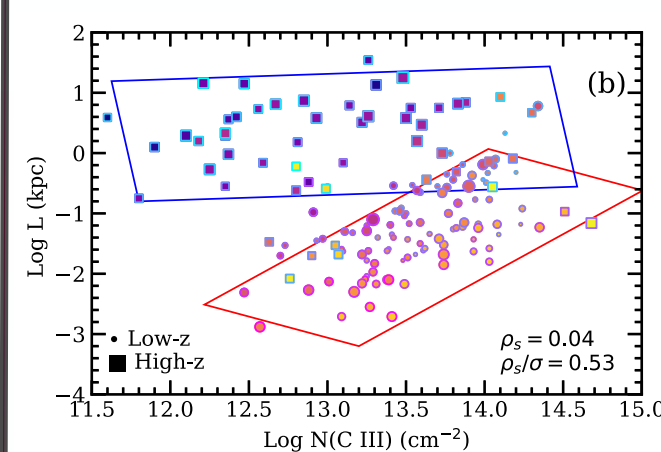


Fig. 5: Size of the absorbers vs. CIII column density shows bimodality in CIII absorbers:

- Clear segregation of two branches of C III absorbers i.e., high-[C/H] (blue hatched boundary) and low-[C/H] branch (red hatched boundary).
- Low-[C/H] branch => mostly from high-z absorbers. High-[C/H] branch => dominantly populated by low-z absorbers.

METALLICITY EVOLUTION AND COMPARISON

- High-[C/H] branch: sub-Damped Lyman Alpha systems (S-DLAs)
- Low-[C/H] branch: partial Lyman limit systems (pLLS) + Lyman limit systems (LLS)

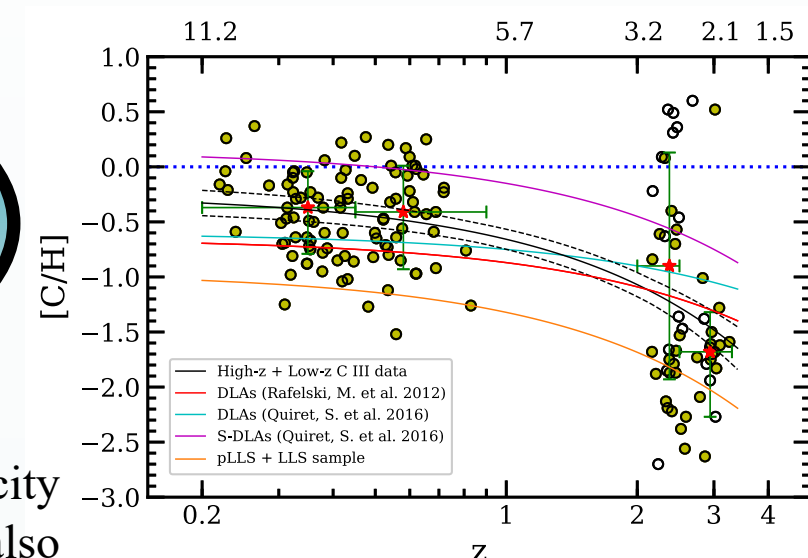


Fig. 6: Significant redshift evolution of metallicity of C III absorbers. The metallicity evolution is also comparable with other class of quasar absorption systems.

Quasar Absorption-GALaxy Survey (QA-GALS)

Our code QA-GALS ((work-in-progress)) has two parts:

- First: identifies nearby galaxies from SDSS DR16 from a user defined impact parameter with respect to the absorber. Cross matches with other available photometric observations from GALEX, PAN-STARRS, WISE catalog.
- Second: runs the SED fitting tool BAGPIPES (Carnall+2018) to obtain the detected galaxy properties such as redshift, age, stellar mass, star formation rate (SFR) and specific star formation rate (sSFR).

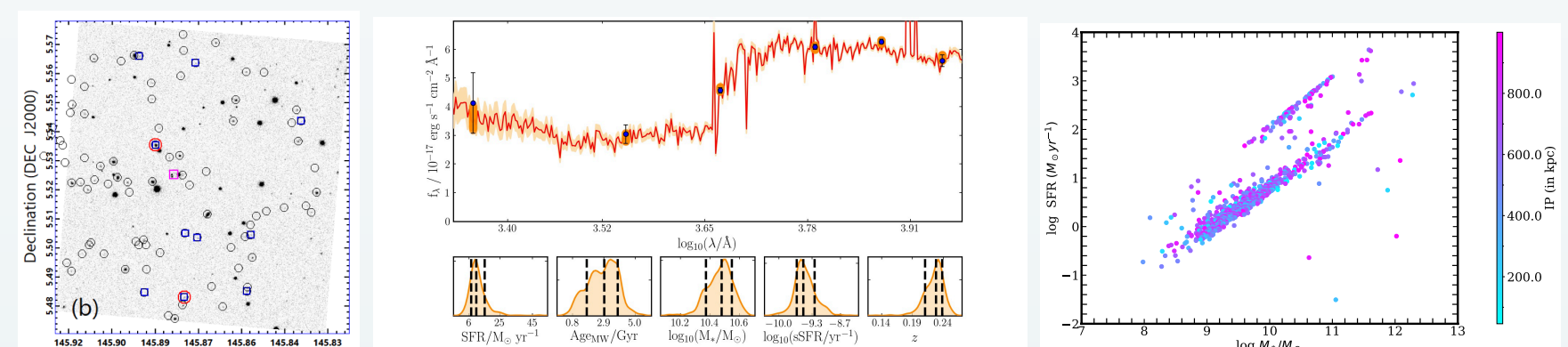


Fig. 7: Left: Galaxies along the quasar sightline J094331.61+053131.4 (magenta square) with an absorber at $z_{\text{abs}} = 0.229019$. Middle: SED fitting outputs for one of the galaxy around the absorber. Right: SFR vs. stellar mass of all the detected galaxies within an impact parameter of 600 kpc around the quasar sightlines.

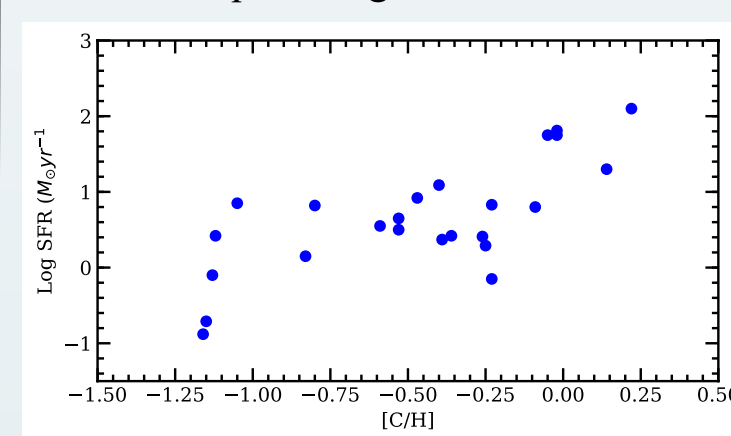


Fig. 8: Absorber-Galaxy connection: SFR of the galaxy vs. metallicity of the absorbers for confirmed galaxy association (dispersion velocity between galaxy and absorber is less than 500 km/s).

Follow-up spectroscopy observations of these quasar fields is needed to put a strong constraint on the redshift of these galaxies!

SUMMARY

- Complete physical properties and evolution of CIII absorbers at low- and high-z.
- Size metallicity relationship can be well explained using cooling time scale.
- Evidence of bimodality in CIII absorbers but needs to be confirmed with uniform sample
- Redshift evolution of metallicity of CIII absorbers is steeper compared to cosmic metallicity evolution of DLAs but consistent with that of sub-DLAs.
- Metallicity of CIII absorbers shows a strong correlation with the SFR of the host galaxies.

REFERENCES

• Carnall et al., 2018, MNRAS, 480, 4379	• Lehner N. et al., 2016, ApJ, 833, 283	• Rafelski M. et al., 2012, ApJ, 559, 507
• Ferland G. J., et al., 2017, RMAA, 53, 385	• Mohapatra A. et al., 2019, MNRAS, 484, 5028	• Quirot S. et al., 2016, MNRAS, 458, 4074
• Khaire V., Srianand R., 2019, MNRAS, 484, 4174	• Mohapatra A. et al., 2021, MNRAS, 501, 5424	• Tumlinson J. et al., 2017, ARA&A, 55, 389
		• Wotta C.B. et al., 2019, ApJ, 872, 81